A simplified mathematical approach for the evaluation of the stabilizing forces applied by a passive cemented bolt to a sliding rock block

A simplified mathematical approach for the evaluation of the stabilizing forces applied by a passive cemented bolt to a sliding rock block

Pierpaolo Oreste[1], Giovanni Spagnoli[2]*

[1] Department of Environmental, Land and Infrastructure Engineering, Politecnico di Torino, Corso Duca Degli Abruzzi 24, 10129 Torino, Italy, *pierpaolo.oreste@polito.it*
ORCID: 0000-0001-8227-9807

[2] BASF Construction Solutions GmbH, Dr-Albert-Frank-Strasse 32, 83308 Trostberg, Germany, *corresponding author, Tel: +49 8621 86-3702,
giovanni.spagnoli@basf.com ORCID: 0000-0002-1866-4345

Abstract

Passive bolting is used to stabilise unstable rock blocks in surface and underground structures due to the various advantages it offers. Despite its use, the design phase still presents aspects of considerable complexity because the fact that the load of the bolt and therefore, its static action depends on its interaction with the block and the stable rock. In the present work, a mathematical model was developed which is capable of directly calculating the stabilisation forces as a function of the characteristic parameters of the bolt and of its interaction with the rock. This discussion is based on a simplified hypothesis of bolt behaviour, which provides negligible errors, and on the observation that the critical point is positioned at the intersection of the bolt with one of the lateral surfaces that separate it from the portion of stable rock. The formulation of the stabilisation forces obtained made it possible to evaluate the static contribution of each single bolt to the stability of the rock block, by varying the diameter of the steel bar and then designing the bolting operation to achieve acceptable stability conditions for the rock block. The application of stabilising equations to a real case, for which the results of load tests on bolt tests were available, allowed us to outline steps to be taken in the bolt design process.

Keywords: rock bolt; Winkler spring approach; rock block stabilisation; safety factor; bolt-rock relative displacement.

Abbreviations and nomenclature

A_{bar}	Area of the section of the steel bar constituting the bolt
$(EA)_{bolt}$	Axial stiffness of the bolt
$(EA)_{bolt,test}$	Axial stiffness of the tested bolt
E_{binder}	Elastic modulus of the binder surrounding the steel bar in the hole
$(EJ)_{bolt}$	Bending stiffness of the bolt
$(EJ)_{bolt,test}$	Bending stiffness of the tested bolt
E_{st}	Steel elastic modulus
$F_{s,yield}$	Safety factor of the bolt with respect to the tensile failure of the steel bar
$F_{s,slip}$	Safety factor of the failure of the bolt-rock interface due to the bolt sliding
$H_{1,I}$	Integration constant in the axial rock-bolt interaction
$H_{2,I}$	Integration constant in the axial rock-bolt interaction
$H_{1,II}$	Integration constant in the axial rock-bolt interaction
$H_{2,II}$	Integration constant in the axial rock-bolt interaction
J_{bar}	Moment of inertia of the steel bar constituting the bolt
k	Ratio between the normal pressure, p, which is applied on the perimeter of the bolt (on the wall of the hole) by the surrounding rock and the normal displacements, y, of the bolt
L_a	Bolt length inside the unstable block
L_p	Bolt length in the stable rock behind the unstable block
L_{test}	Length of the tested bolt
M	Bending moment in the bolt
N	Axial force in the bolt
$N_{0,max}$	Bolt stabilising force in the direction of the bolt axis

N_{test}	Tensile axial force applied at the bolt head from pull-out tests
N_{yield}	Force causing the bar failure under tensile stress
N_{slip}	Force causing the bolt-rock interface to fail for a unit bolt length
$N_{slip,test}$	Force causing the bolt-rock interface of the test bolt to fail (i.e., bolt slips away)
N_0	Value of the tensile force in the axial direction of the bolt on the intersection point between the bolt and a block surface
p	Value of the normal pressure (perpendicular to the axial direction) applied on the lateral surface of the bolt
P_{hole}	Perimeter of the cross-section of the bolt
$P_{hole,test}$	Perimeter of the cross-section of the tested bolt
S_{bar}	Static moment of the half section of the bar with respect to the barycentric axis
T	Shear force in the bolt
t_{binder}	Thickness of the binder annulus surrounding the steel bar
T_0	Value of the shear force perpendicular to the axial direction of the bolt on the intersection point between the bolt and a block surface
$T_{0,max}$	Bolt stabilising force in the transverse direction
T_{test}	Force perpendicular to the axis of the bolt in correspondence to its head from lateral shear tests
v_r	Value of the relative axial displacement between the bolt and the surrounding rock
y	Normal displacements of the bolt perpendicular to the axial direction of the bolt

α	Parameter characterising the interaction in the axial direction between the bolt and the surrounding rock $\alpha = \sqrt{\frac{\beta_c \cdot P_{hole}}{EA}}$
β	Parameter characterising the interaction in the transverse direction between the bolt and the surrounding rock $\beta = \sqrt[4]{\frac{k \cdot \Phi_{hole}}{4 \cdot EJ}}$
β_c	Ratio between the shear stresses, τ, that develop on the perimeter of the bolt and the relative axial displacements, v_r
δ	Arbitrary displacement of the block
δ_n	Displacement component of the block in the axial direction of the bolt
$\delta_{n,test}$	Bolt head axial displacement due to the application of the axial force, N_{test}
δ_t	Displacement component of the block in the transverse direction of the bolt
$\delta_{t,test}$	Transverse bolt head displacement due to the application of a shear force, T_{test}
Φ_{bar}	Diameter of the steel bar
Φ_{hole}	Diameter of the hole (of the bolt)
$\Phi_{hole,test}$	Diameter of the tested bolt
χ	Adimensional parameter for the evaluation of the stabilising forces
λ	Adimensional parameter for the evaluation of the stabilising forces
η	Adimensional parameter for the evaluation of the stabilising forces
ω	Adimensional parameter for the evaluation of the stabilising forces
ψ	Adimensional parameter for the evaluation of the stabilising forces
ϱ	Adimensional parameter for the evaluation of the stabilising forces
σ_{yield}	Steel yield stress

σ_{id}	Ideal stress which accounts for the simultaneous presence of an axial and a shear stress in the same section of the steel bar
τ	Shear stress on the lateral surface of the bolt
τ_{lim}	Ultimate limit shear stress of the rock-bolt interface
$\tau_{0,I}$	Existing shear stress for x=0 (at the intersection with a lateral surface of the rock block) on the side of the potentially unstable rock block
$\tau_{0,II}$	Existing shear stress for x=0 (at the intersection with a lateral surface of the rock block) on the side of the portion of stable rock
ξ	Adimensional parameter for the evaluation of the stabilising forces

Introduction

Passive rock bolts (Fig. 1), which have zero initial load, are normally used to prevent rock blocks from falling or sliding. The mobilised stabilising load increases with the displacement of the potentially unstable rock block. Among the different types of passive rock anchors, fully-grouted rock bolts which rely on a binder that fills the annulus between the element and the borehole wall (Bawden, 2011) are normally used in practice and are able to support tensile, compressive, shear, and bending loads (Ghadimi et al. 2015).

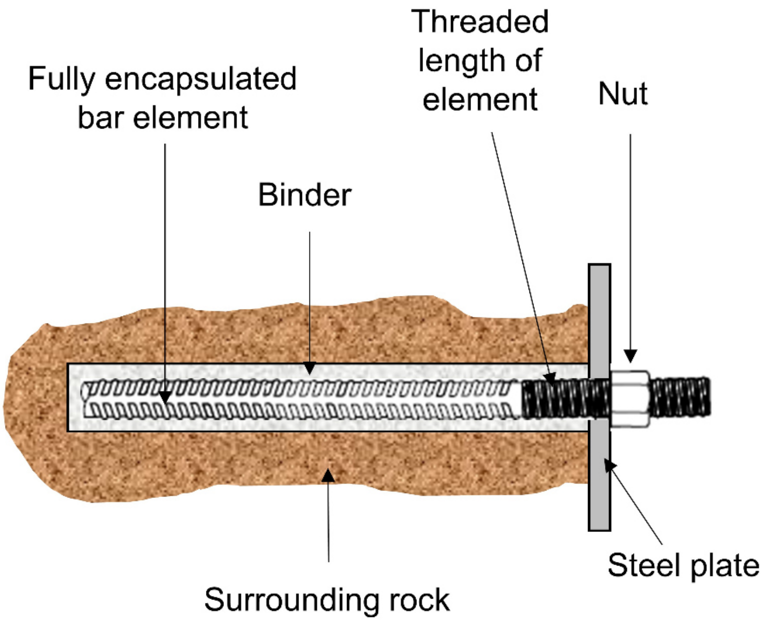

Fig. 1 Sketch of a passive rock bolt.

As a result of the rock bolt deformation, a normal and a shear force act on the rock mass and restrain further deformation of the rock, transferring loads from the stable to the unstable rock mass (Nie et al. 2014). Rock bolts are used in both low and high in situ stress conditions (Li, 2017). In heavily jointed rocks, they create a ‘reinforced arch’ around an underground opening, thereby providing stability to the cavity (Lang, 1961) as the bolt action increases due to an increase in axial shear forces and bending moments in the bolt rod (e.g., ; Oreste, 2009; Oreste and Dias 2012; Ranjbarnia et al., 2014, 2016). Rock bolts improve the stiffness of rocks (Chappell, 1989). The main factors affecting the shear strength of rock bolts are the materials they are made of, the size of the rod body, and the type of rock mass (Ferrero, 1995).

Several analytical and numerical methods are found in the literature describing complex bolt-grout-rock interactions and suggesting improvements to bolt geometry, grout properties, or the interaction between the two (e.g., Blümel et al. 1997; Aziz and Jalalifar 2007; Osgoui and Oreste 2007; Das and Deb 2011; Aminaipour 2012; Oreste 2013; Chen et al. 2015; Changxing et al. 2015; Chang et al. 2017). However, many of the methods found and described in the literature, with all their advantages and limitations, are too complex to use for conventional design analysis. In particular, the analysis of the behaviour of passive bolts used to stabilise a potentially unstable rock block that slides along one or more surfaces is complex. In this case, the passive bolts were initially unloaded and even a slight movement (sometimes imperceptible) could activate them, causing forces to develop along their axes and forces to be transferred to the block capable of stabilising it.

This analysis can be done using numerical tools, but it requires rather long calculations and it is necessary to operate in a three-dimensional environment. An easier way to study the problem is to consider the bolt-rock interactions, both in the transverse and axial directions, using the Winkler spring approach (Oreste and Cravero, 2008; Oreste, 2009). In this way, the interaction phenomenon was studied in the elastic field and it was possible to quickly determine the stabilising forces of the bolt by evaluating the limits under the same operating conditions. Even this solution, however, requires a numerical solution to cope with the significant number of unknowns and the different boundary conditions that must be considered in order to characterise the behaviour of the bolt. The analysis of the behaviour of passive bolts in a number of practical cases in which a bolt is needed to stabilise a block of potentially unstable rock and knowledge of the variability intervals of the parameters influencing the bolt-rock interaction allowed us to identify the critical points at which the bolt intersects with a lateral surface of the rock block.

In addition, some simplified hypotheses on the behaviour of the bolt with respect to the transverse interaction with the surrounding rock have produced negligible errors and can significantly simplify the mathematical model. In this paper, we review the fundamental equations that govern bolt-rock interactions using according to the independent Winkler springs approach. The development of the mathematical model is explained in order to achieve the stabilisation forces that the bolts apply to prevent a potentially unstable block from sliding along one or more surfaces that separate it from stable rock. The fundamental parameters influencing these stabilisation forces are analysed in order to speed up the design of the operations needed to stabilise a rock block with the necessary safety factors. A practical application to a real case allowed us to delineate the process of determining the influencing parameters and assessing the stabilisation forces as the diameter of the steel bar that constitutes the bolts varies.

Mathematical development of the simplified approach

Oreste and Cravero (2008) developed a mathematical procedure to calculate the stabilising forces applied by a passive bolt to a rock block and studied the effect of an axial displacement and a lateral displacement of the block with respect to the direction of the bolt axis. The direction of the displacement vector of the rock block was initially determined on the basis of the orientation of the sliding surface, in particular of the orientation of the line of intersection of the sliding surfaces.

Then the angle ϑ, which is the angle of the block displacement vector with the direction of the axis of the passive bolts, was estimated (Oreste, 2009). In underground applications, the bolts are generally arranged horizontally and perpendicular to the cavity wall where there is a rock block which is potentially unstable due to sliding along one or more natural discontinuities present in the rock mass.

The axial component, δ_n, and the transversal component, δ_t, of a generic displacement of the rock block, δ, are obtained from the following equations, respectively:

$$\delta_n = -\delta \cdot cos(\vartheta) \quad (1)$$

$$\delta_t = \delta \cdot sin(\vartheta) \quad (2)$$

The effect of the axial component is to create a displacement of the block in the direction of the bolt axis, with respect to the stable rock present at its contour. The effect of the transversal component is to create a relative displacement of the block in the direction perpendicular to the axis of the bolt, with respect to the stable rock present at its contour (Fig. 2).

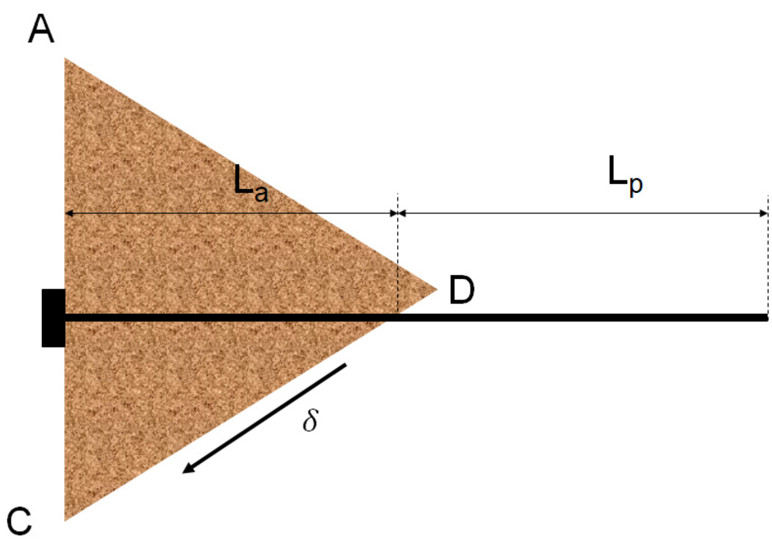

Fig. 2 Schematic representation of the potentially unstable rock block and the passive bolt (not to scale). L_a and L_p are the lengths of the bolt inside the

potentially unstable rock block (zone I) and in the stable rock (zone II), respectively, ϑ is the angle of the block displacement vector with the direction of the axis of the passive bolts.

From the analysis of the axial component of the displacement, δ_n, it is possible to obtain the trend of the axial force, N, along the bolt and the relative displacement v_r of the steel bar with respect to the surrounding rock and the shear stresses, τ, developing at the interface between the bolt and the rock.

In more detail, the trend of the axial force N for the two areas in which the bolt is divided were obtained from the following expressions:

Within the rock block (zone I): $N = (EA)_{bolt} \cdot \alpha \cdot \left(H_{1,I} \cdot e^{\alpha x} - H_{2,I} \cdot e^{-\alpha x}\right)$ (3)

In the stable rock (zone II): $N = (EA)_{bolt} \cdot \alpha \cdot \left(H_{1,II} \cdot e^{\alpha x} - H_{2,II} \cdot e^{-\alpha x}\right)$ (4)

Where:

$$H_{1,I} = -\delta_n \cdot \frac{\left(1-e^{-2\cdot\alpha\cdot L_p}\right)\cdot e^{-2\cdot\alpha\cdot L_a}}{2\cdot\left[1+e^{-2\cdot\alpha\cdot(L_a+L_p)}\right]} \tag{5}$$

$$H_{2,I} = \delta_n \cdot \frac{\left(1-e^{-2\cdot\alpha\cdot L_p}\right)}{2\cdot\left[1+e^{-2\cdot\alpha\cdot(L_a+L_p)}\right]} \tag{6}$$

$$H_{1,II} = \delta_n \cdot \frac{\left(1+e^{-2\cdot\alpha\cdot L_a}\right)\cdot e^{-2\cdot\alpha\cdot L_p}}{2\cdot\left[1+e^{-2\cdot\alpha\cdot(L_a+L_p)}\right]} \tag{7}$$

$$H_{2,II} = \delta_n \cdot \frac{\left(1+e^{-2\cdot\alpha\cdot L_a}\right)}{2\cdot\left[1+e^{-2\cdot\alpha\cdot(L_a+L_p)}\right]} \tag{8}$$

L_a and L_p are the lengths of the bolt inside the potentially unstable rock block (zone I) and in the stable rock (zone II), respectively, and their sum is the total length of the bolt; α is a parameter characterising the interaction in the axial direction between bolt and rock as:

$$\alpha = \sqrt{\frac{\beta_c \cdot P_{hole}}{(EA)_{bolt}}} \tag{9}$$

$(EA)_{bolt}$ is the axial stiffness of the bolt, evaluated as:

$$(EA)_{bolt} = E_{st} \cdot \left(\frac{\pi}{4} \cdot {\Phi_{bar}}^2\right) + E_{binder} \cdot \left[\frac{\pi}{4} \cdot \left({\Phi_{hole}}^2 - {\Phi_{bar}}^2\right)\right] \quad (10)$$

Where:

Φ_{bar} is the bar diameter;

E_{st} is the steel elastic modulus;

E_{binder} is the elastic modulus of the binder surrounding the steel bar in the hole;

P_{hole} is the perimeter of the cross-section of the bolt;

β_c is the ratio between the shear stresses developing on the perimeter of the bolt (on the wall of the hole), τ, and the relative axial displacements, v_r. β_c depends in general on the characteristics of the material surrounding the steel bar and on the elastic modulus of the rock;

Φ_{hole} is the diameter of the hole where the bolt is inserted as $\Phi_{hole} = \Phi_{bar} + 2 \cdot t_{binder}$; and

t_{binder} is the thickness of the binder annulus around the steel bar.

The distance x, measured along the bolt axis, originates at the intersection point of the bolt with one of the block discontinuities (block surfaces). The shear stress, τ, on the lateral surface of the bolt is given by the following equations:

Within the rock block (zone I): $\tau = -\beta_c \cdot \left(H_{1,I} \cdot e^{\alpha x} + H_{2,I} \cdot e^{-\alpha x}\right)$ (11)

In the stable rock (zone II): $\tau = -\beta_c \cdot \left(H_{1,II} \cdot e^{\alpha x} + H_{2,II} \cdot e^{-\alpha x}\right)$. (12)

By analysing the transverse component of the displacement δ_t, it is possible to obtain the trend of the shear force T along the bolt, the transverse displacement of the bolt y (in the direction perpendicular to its axis), and the bending moment M.

It has been noted by an extensive parametric analysis adopting input parameters within ranges of variability typical of all possible cases which can be encountered in practice that it is possible to adopt a simplified approach referring to the hypothesis of infinite bolt length in the two considered zones (zone I and zone II) making negligible errors (below 1%) (Oreste et al., 2020).

In more detail, the trend of the shear force T, according to this simplified approach, was obtained from the following expression valid for both areas (zone I and II):

$$T = (EJ)_{bolt} \cdot \beta^3 \cdot \delta_t \cdot e^{-\beta x} \cdot \left(cos(\beta x) - sin(\beta x)\right) \tag{13}$$

In the same way, the trend of the moment M along the bolt is given by the following equation:

$$M = (EJ)_{bolt} \cdot \beta^2 \cdot \delta_t \cdot e^{-\beta x} \cdot sin(\beta x) \tag{14}$$

Where:

$(EJ)_{bolt}$ is the bending stiffness of the bolt, evaluated on the basis of the following equation:

$$(EJ)_{bolt} = E_{st} \cdot \left(\frac{\pi}{64} \cdot \Phi_{bar}{}^4\right) + E_{binder} \cdot \left[\frac{\pi}{64}\left(\Phi_{hole}{}^4 - \Phi_{bar}{}^4\right)\right] \tag{15}$$

and β is the parameter that characterises the interaction in the transverse direction between bolt and rock:

$$\beta = \sqrt[4]{\frac{k \cdot \Phi_{hole}}{4 \cdot (EJ)_{bolt}}} \tag{16}$$

where k is the ratio between the normal pressure, p, which is applied on the perimeter of the bolt by the surrounding rock, and the transversal displacement, y, of the bolt. The critical point along the bolt is identified at the intersection with a potentially unstable rock block side surface (x = 0). At that point, the stress state inside the bar and on the bolt-rock interface is high. It is therefore useful to be able to evaluate the stress characteristics of the forces N and T, and the shear stress value τ for x = 0, considering that M_0 (M for x=0) is zero:

$$N_0 = (EA)_{bolt} \cdot \alpha \cdot \left(H_{1,I} - H_{2,I}\right) \tag{17}$$

$$T_0 = (EJ)_{bolt} \cdot \beta^3 \cdot \delta_t \tag{18}$$

$$\tau_{0,I} = -\beta_c \cdot (H_{1,I} + H_{2,I}) \quad (19)$$

$$\tau_{0,II} = -\beta_c \cdot (H_{1,II} + H_{2,II}) \quad (20)$$

From the previous equations it is possible to derive the safety factor of the bolt with respect to the tensile failure of the steel bar ($F_{s,yield}$) and to the failure of the bolt-rock interface due to the bolt sliding ($F_{s,slip}$):

$$F_{s,yield} = \frac{\sigma_{yield}}{\sigma_{id}} \quad (21)$$

$$F_{s,slip} = \frac{\tau_{lim}}{\tau_{0,II}} \quad (22)$$

Where:

σ_{yield} is the yield stress of steel;

τ_{lim} is ultimate limit shear stress of the interface rock-bolt;

$\tau_{0,II}$ is the existing shear stress for x=0 (at the intersection with a lateral surface of the rock block) on the side of the portion of stable rock; this stress is greater than the analogous stress existing on the side of the potentially unstable rock block ($\tau_{0,I}$); and

σ_{id} is the ideal stress which takes into account the simultaneous presence of an axial and a shear stress in the section of the steel bar as expressed by:

$$\sigma_{id} = \sqrt{\left(\frac{N_0}{A_{bar}}\right)^2 + 3 \cdot \left(\frac{T_0 \cdot S_{bar}}{\Phi_{bar} \cdot J_{bar}}\right)^2} \quad (23)$$

Where:

A_{bar} is the area of the section of the steel bar constituting the bolt ($A_{bar} = \pi \cdot \frac{\Phi_{bar}^2}{4}$);

S_{bar} is the static moment of the half section of the bar with respect to the barycentric axis $S_{bar} = \frac{1}{12} \cdot \Phi_{bar}^3$;

J_{bar} is the moment of inertia of the steel bar constituting the bolt, $J_{bar} = \pi \cdot \frac{\Phi_{bar}^4}{64}$;

By setting the values of the safety factors equal to the minimum values considered admissible for the two failure mechanisms considered ($F_{s,yield}$=$F_{s,adm,yield}$

and $F_{s,slip} = F_{s,adm,slip}$) and by substituting, it is possible to obtain the following equations of the maximum forces T_0 and N_0. Referring to the failure of the steel bar at the point of intersection with the block surface (x=0):

$$T_{0,max} = \frac{N_{yield}}{F_{s,adm,yield}} \cdot \frac{2}{\sqrt{\left[\frac{(EA)_{bolt} \cdot \alpha}{(EJ)_{bolt} \cdot \beta^3}\right]^2 \cdot \left[\frac{(1+e^{-2\alpha L_a}) \cdot (1-e^{-2\alpha L_p})}{\left(1+e^{-2\alpha(L_a+L_p)}\right)}\right]^2 \cdot \frac{1}{tan^2(\vartheta)} + \frac{64}{3}}} \tag{24}$$

$$N_{0,max} = \frac{N_{yield}}{F_{s,adm,yield}} \cdot \frac{1}{\sqrt{1+\frac{64}{3} \cdot \left[\frac{(EJ)_{bolt} \cdot \beta^3}{(EA)_{bolt} \cdot \alpha}\right]^2 \cdot \left[\frac{\left(1+e^{-2\alpha(L_a+L_p)}\right)}{(1+e^{-2\alpha L_a}) \cdot (1-e^{-2\alpha L_p})}\right]^2 \cdot tan^2(\vartheta)}} \tag{25}$$

Where:

N_{yield} is the force causing bar failure under a tensile stress $N_{yield} = \sigma_{yield} \cdot A_{bar}$.

Referring to the failure of the bolt-rock interface at the point of intersection with the surface of the block (x = 0), with reference to the side on the stable rock, where shear stress τ is higher:

$$T_{0,max} = 2 \cdot \frac{N_{slip}}{F_{s,adm,slip}} \cdot \left[\frac{(EJ)_{bolt} \cdot \beta^3}{(EA)_{bolt} \cdot \alpha}\right] \cdot \left[\frac{\left(1+e^{-2\alpha(L_a+L_p)}\right)}{(1+e^{-2\alpha L_a}) \cdot (1+e^{-2\alpha L_p})}\right] \cdot \frac{1}{\alpha} \cdot tan(\vartheta) \tag{26}$$

$$N_{0,max} = \frac{N_{slip}}{F_{s,adm,slip}} \cdot \frac{1}{\alpha} \cdot \left[\frac{(1-e^{-2\alpha L_p})}{(1+e^{-2\alpha L_p})}\right] \tag{27}$$

Where:

N_{slip} is the force which causes the bolt-rock interface to fail for a unit bolt length $N_{slip} = \tau_{lim} \cdot \pi \cdot \Phi_{hole}$.

The forces shown above represent the maximum forces that can be reached when the safety factors of the bolt, in the two failure mechanisms considered, reach the minimum allowable values. In practice, they are the maximum forces that can be achieved with the movement of the rock block, while keeping the bolt in safe operating condition. Verification against the two failure mechanisms must take place simultaneously, and therefore, it was necessary to consider the minimum value between the two pairs of forces:

$$T_{0,max} = min\left(\frac{N_{yield}}{F_{s,adm,yield}} \cdot \frac{2}{\sqrt{\frac{\lambda^2 \cdot \chi^2}{tan^2(\vartheta)}+\frac{64}{3}}} \; ; \; \frac{N_{slip}}{F_{s,adm,slip}} \cdot \frac{2 \cdot tan(\vartheta)}{\lambda \cdot \psi \cdot \alpha}\right) \tag{28}$$

$$N_{0,max} = min\left(\frac{N_{yield}}{F_{s,adm,yield}} \cdot \frac{1}{\sqrt{1+\frac{64}{3} \cdot \frac{tan^2(\vartheta)}{\lambda^2 \cdot \chi^2}}} \; ; \; \frac{N_{slip}}{F_{s,adm,slip}} \cdot \frac{\omega}{\alpha}\right) \tag{29}$$

Where:

$$\lambda = \left[\frac{(EA)_{bolt} \cdot \alpha}{(EJ)_{bolt} \cdot \beta^3}\right] \tag{30}$$

$$\chi = \left[\frac{\left(1+e^{-2\alpha L_a}\right) \cdot \left(1-e^{-2\alpha L_p}\right)}{\left(1+e^{-2\alpha (L_a+L_p)}\right)}\right] \tag{31}$$

$$\psi = \left[\frac{\left(1+e^{-2\alpha L_a}\right) \cdot \left(1+e^{-2\alpha L_p}\right)}{\left(1+e^{-2\alpha (L_a+L_p)}\right)}\right] \tag{32}$$

$$\omega = \left[\frac{\left(1-e^{-2\alpha L_p}\right)}{\left(1+e^{-2\alpha L_p}\right)}\right] \tag{33}$$

The forces obtained are of interest because they are the maximum values of axial and shear forces that can be achieved along the bolt (in particular at the point of intersection of the bolt with a lateral surface of the block). They also represent the stabilising forces that the single bolt applies to the potentially unstable rock block in the direction of the bolt axis ($N_{0,max}$) and in the transverse direction (perpendicular to the bolt axis). This plane includes the block displacement vector (i.e., the intersection line of the sliding surfaces) and the bolt axis ($T_{0,max}$).

Analysis of the stabilising forces of the passive bolt

The stabilisation forces were evaluated starting from the limit forces N_{yield} and N_{slip} (which caused the two failure mechanisms described above) and the respective minimum safety factors considered acceptable. It is also necessary to know the angle that the displacement vector of the block forms with the axis of the bolt (ϑ) and the stiffness parameters λ and α. Other parameters that link the stiffness parameters to the geometric ones (L_a and L_p) are necessary for the calculation of χ, ψ, and ω.

Figures 3 through 9 show graphs of the dimensionless parameters λ, χ, ψ, and ω with changing stiffness value α for different bar diameters Φ_{bar}, L_a, and L_p and for the stiffness parameter β. The values of bolt length and diameter adopted in the mathematical model are assumed on the basis of values available in the literature (e.g., Bawden, 2011; DSI, 2015).

The graphs were obtained considering t_{binder} equal to 10 mm, E_{steel} equal to 210 GPa, and E_{binder} equal to 25 GPa. From the analysis of the figures, it is possible to detect how for α > 5, the parameters χ and ψ can be set equal to 1; and the parameter ω can be set equal to 1 for α > 2. In all other cases, it is necessary to calculate the values through equations 30–33) or by using the graphs in Figures 3–6; then to proceed with the evaluation of the maximum forces $T_{0,max}$ and $N_{0,max}$ mobilisable by each bolt (eq. 28 and 29). If α > 5, then equations 28 and 29 simplify as follows:

$$T_{0,max} = min\left(\frac{N_{yield}}{F_{s,adm,yield}} \cdot \xi \,;\, \frac{N_{slip}}{F_{s,adm,slip}} \cdot \frac{\eta}{\alpha}\right) \tag{34}$$

$$N_{0,max} = min\left(\frac{N_{yield}}{F_{s,adm,yield}} \cdot \varrho \,;\, \frac{N_{slip}}{F_{s,adm,slip}} \cdot \frac{1}{\alpha}\right) \tag{35}$$

Where:

$$\xi = \frac{2}{\sqrt{\frac{\lambda^2}{tan^2(\vartheta)} + \frac{64}{3}}} \tag{36}$$

$$\eta = \frac{2 \cdot tan(\vartheta)}{\lambda} \tag{37}$$

$$\varrho = \frac{1}{\sqrt{1+\frac{64}{3}\cdot\frac{tan^2(\vartheta)}{\lambda^2}}} \tag{38}$$

For these cases, the length values L_a and L_p do not longer influence the values of the stabilising forces. The path of ξ, η, and ϱ as functions of λ and the angle ϑ are shown in Figures 7–9. The obtained forces ($T_{0,max}$ and $N_{0,max}$) can then be included in the analyses for the block stability and therefore, to design the bolting intervention necessary to achieve stabilisation of the block.

All the parameters mentioned in equations 30–33 and 36–38 are dimensionless and are only useful to better understand the evolution of the coefficients $T_{0,max}$ and $N_{0,max}$ by varying some fundamental parameters in the rock-bolt interaction. The only parameter that has an important physical meaning is λ (eq. 30), which is the ratio between the product of the stiffness parameters referred to the axial interaction divided by the product of the stiffness parameters referred to the transverse interaction between bolt and rock.

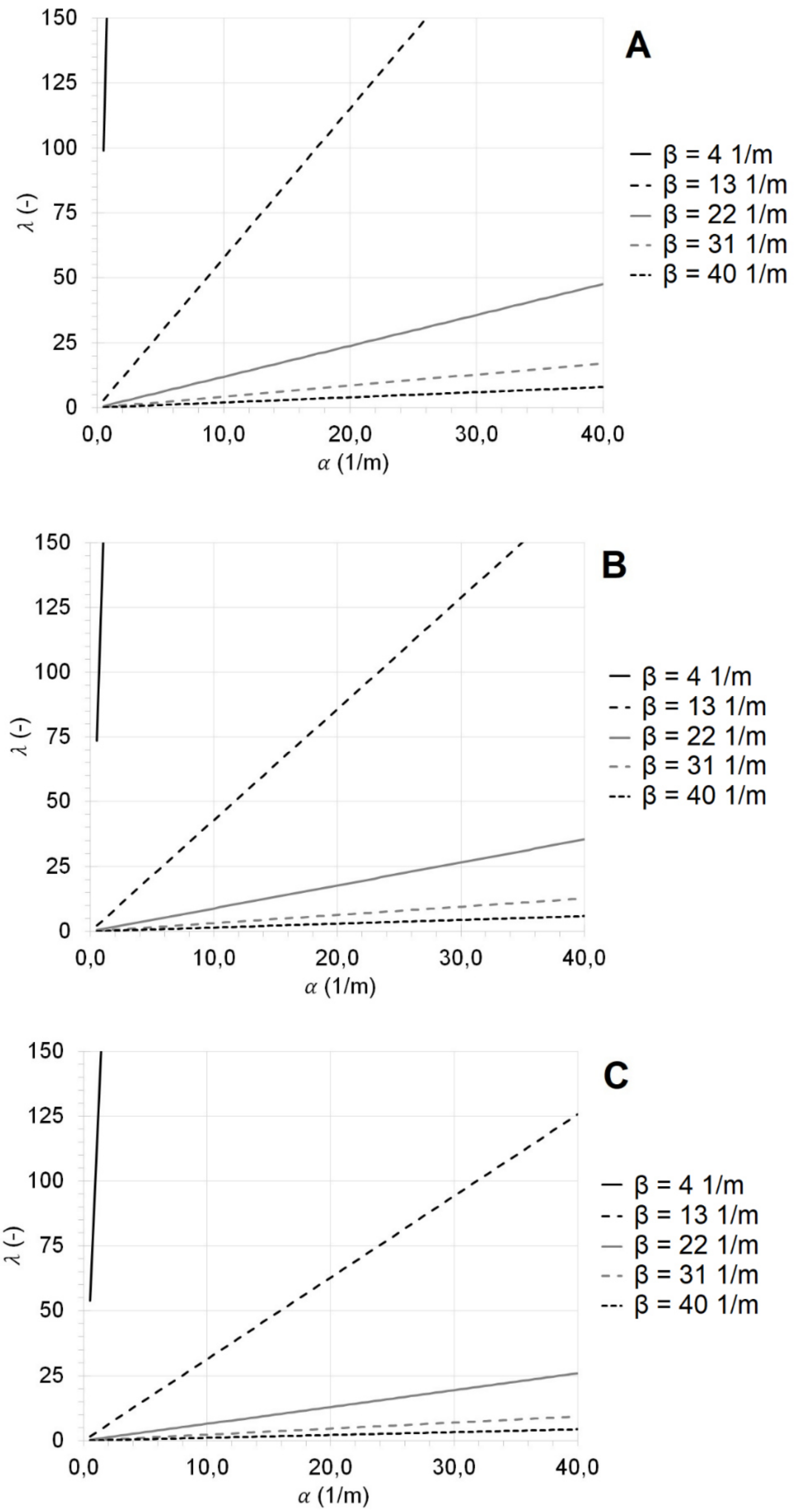

Fig. 3 Trend of the parameter λ by changing α for different values of β. A) Bar diameter 20 mm; B) Bar diameter 28 mm; C) Bar diameter 36 mm.

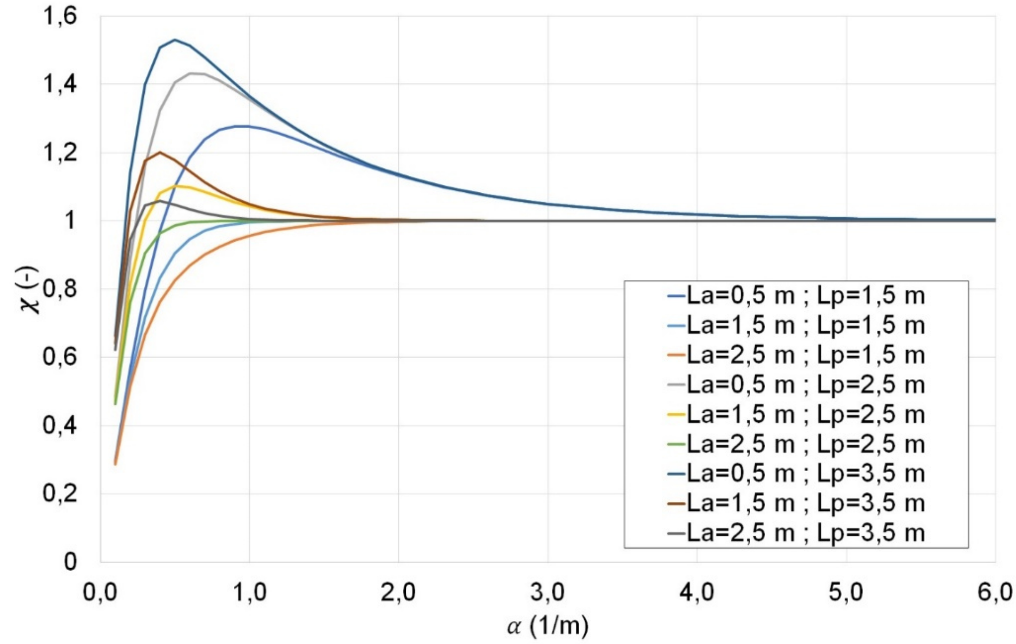

Fig. 4 Trend of the parameter χ by changing α for different values of L_a (bolt section in the potentially unstable rock block) and L_p (bolt section in stable rock).

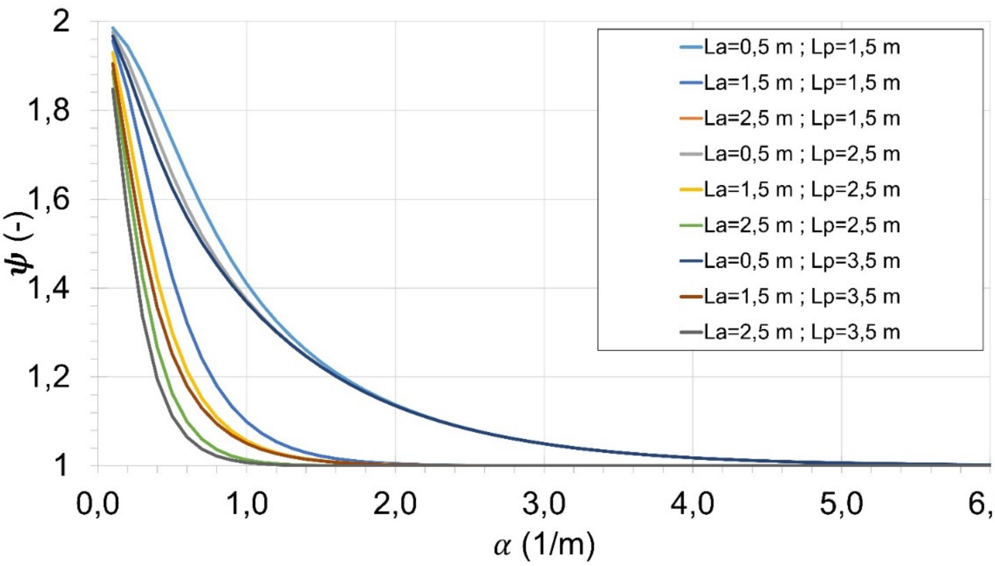

Fig. 5 Trend of parameter ψ by changing α for different values of L_a (bolt section in the potentially unstable rock block) and L_p (bolt section in stable rock). The line with L_a=1.5 m and L_p=2.5 m overlaps the line with L_a=2.5 m and L_p=1.5 m.

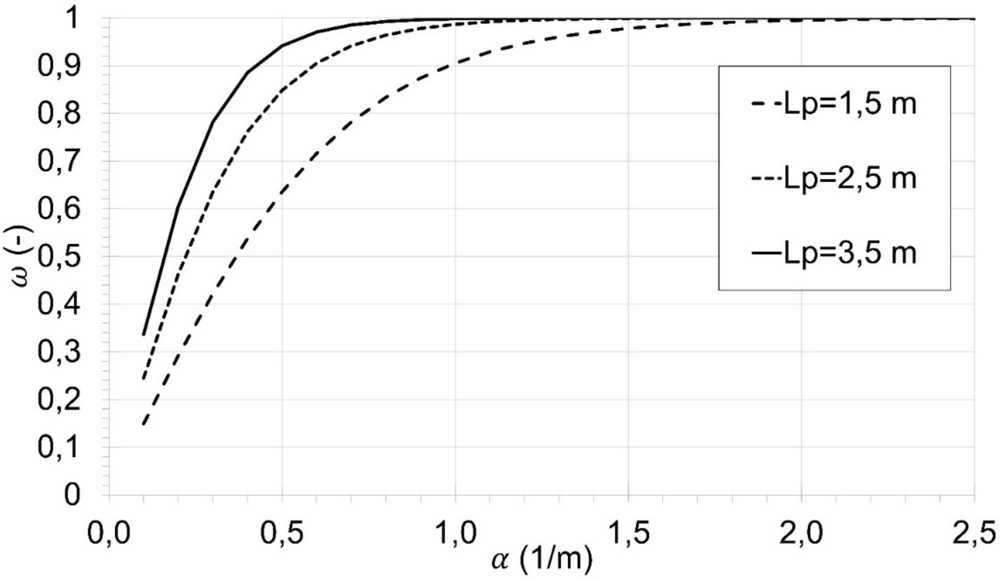

Fig. 6 Trend of the parameter ω for L_a=0.5 m (bolt section in the potentially unstable rock block) and different values of L_p (bolt section in stable rock).

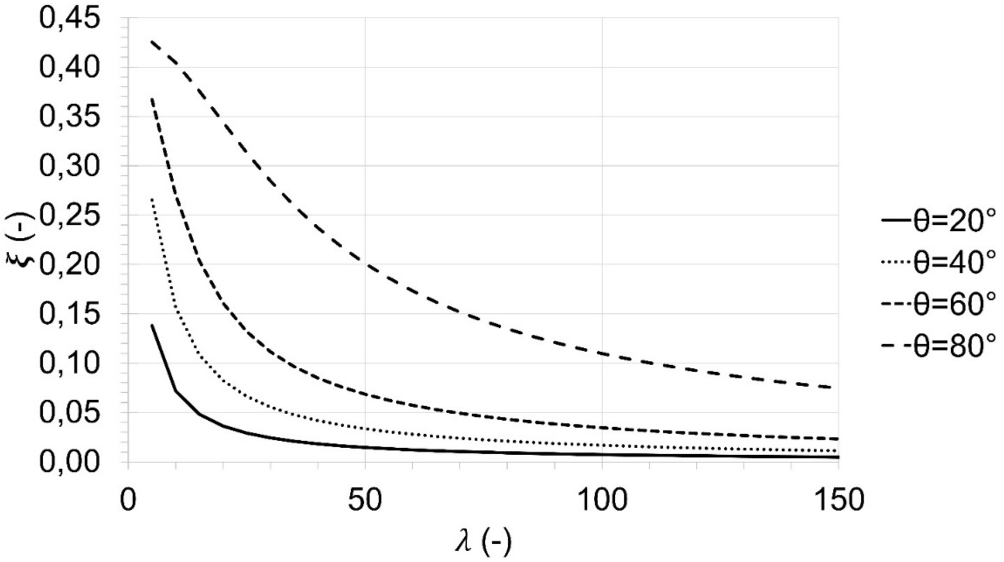

Fig. 7 Trend of the parameter ξ by varying λ for different values of angle ϑ.

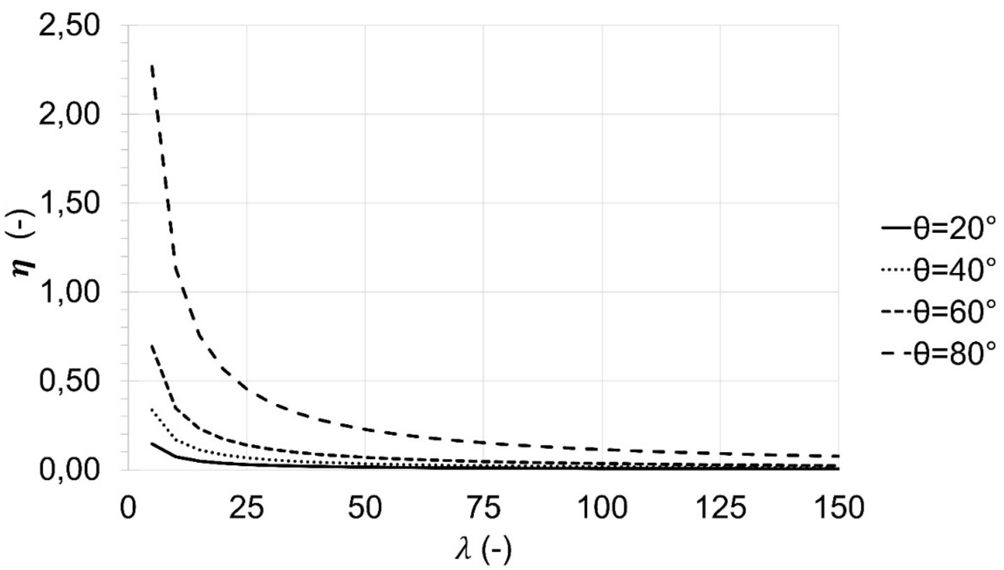

Fig. 8 Trend of the parameter η by varying λ for different values of angle ϑ.

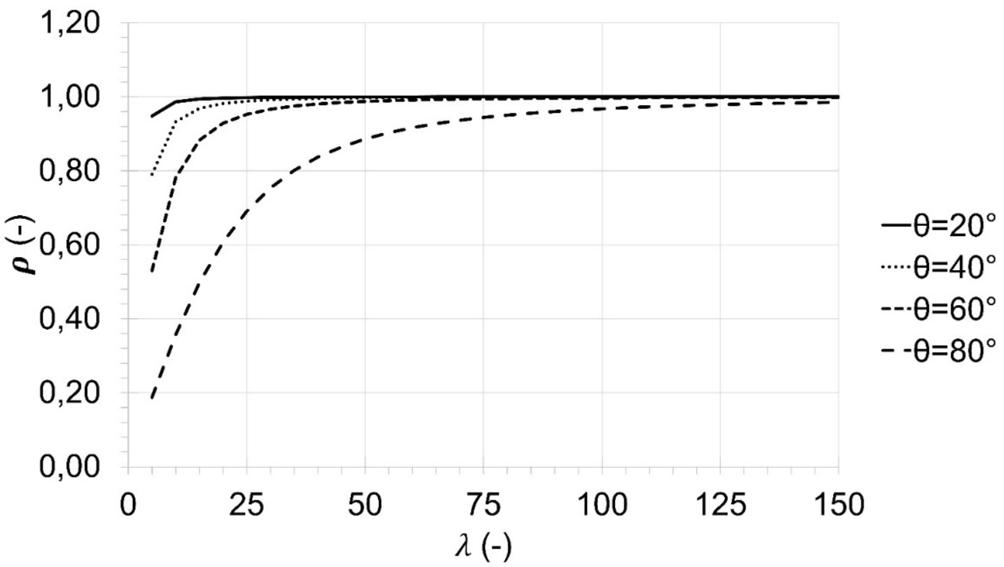

Fig. 9 Trend of the parameter ρ by varying λ for different values of angle ϑ.

Application of the theoretical equations to a real case

Based on the theoretical model discussed above, the importance of the stiffness parameters of the bolt-rock interaction (α and β) on the behaviour of passive bolts is evident (see eq. 9 and 16). These parameters, which have the inverse dimension of length, depend respectively on the axial $(EA)_{bolt}$ (eq. 10) and bending stiffness

$(EJ)_{bolt}$ (eq. 15) of the bolt and on the parameters k and β_c. The parameter k represents the ratio between the normal contact pressure, p, on the external surface of the bolt and the lateral displacement, y, of the bolt in the direction perpendicular to its axis ($p = k \cdot y$). On the other hand, β_c represents the ratio between the shear stress τ developing on the lateral surface of the bolt and the bolt-rock relative displacement v_r in the axial direction ($\tau = \beta_c \cdot v_r$). The parameters k and β_c can be obtained from specific in situ tests on bolts of reduced length (even the diameter may be different from what is intended to be used for the stabilisation of the block). More specifically, k can be obtained from lateral shear tests by applying a force perpendicular to the axis of the bolt in correspondence to its head (T_{test}), while β_c is obtained from pull-out tests of the bolt with the application of a tensile axial force at the bolt head (N_{test}).

The stabilising force equations $N_{0,max}$ and $T_{0,max}$ (eq. 28 and 29) have been applied to the case of a potentially unstable rock block in a limestone formation (mean intact UCS values were about 140 MPa) present near a municipal road in Northern Piedmont (Northern Italy). The block had a planar sliding surface with an inclination of 35° with respect to the horizontal plane. The cement was CEM I 52.5 R with a water/cement ratio, w/c, 0.45, which is typical of anchors in rock (e.g., Littlejohn and Bruce, 1977). The grout was cured for 28 days prior to testing. Transverse load tests and pull-out tests were performed.

The transverse load test (a non-destructive test) was carried out first, until a force compatible with the elastic behaviour of the bolt and its interface with the surrounding rock was reached. In the transverse load test (Fig. 10), a concrete ballast was connected to the bolt head through a rope. A dynamometric device applied stress on the rope and thus applied the test force (T_{test}) to the bolt head. The force was increased in equal intervals until the maximum test force was reached. For each value of the applied force, the displacement of the head $\delta_{t,test}$ was measured in the same direction as the force through high precision strain gauges. It was possible to plot a diagram of T_{test} vs. $\delta_{t,test}$, which identified a straight line that best approximated the experimental points, and to evaluate the angular coefficient which represents the ratio $T_{test}/\delta_{t,test}$. This ratio is useful for estimating the stiffness parameter k (eq. 39) and the stiffness parameter β (eq. 16). In the specific case examined, the transverse load test reached the maximum force of 0.75 tons with four successive load steps of equal value; the final displacement was 0.4 mm. The angular coefficient of the interpolated straight line was found to be approximately 18.4 MN/m. It was taken as the $T_{test}/\delta_{t,test}$ (eq. 39), from which the value of the stiffness parameter, k, in the transverse interaction bolt-rock was estimated. The ratio between the applied force and the measured lateral displacement allowed us to obtain the parameter k from the following equation:

$$k = \frac{\sqrt[3]{4}}{\Phi_{hole,test} \cdot \sqrt[3]{(EJ)_{bolt,test}}} \cdot \left(\frac{T_{test}}{\delta_{t,test}}\right)^{\frac{4}{3}} \qquad (39)$$

Where:

$\delta_{t,test}$ is the lateral bolt head displacement due to the application of a lateral shear force, T_{test};

$\Phi_{hole,test}$ is the diameter of the tested bolt; and

$(EJ)_{bolt,test}$ is the bending stiffness of the tested bolt.

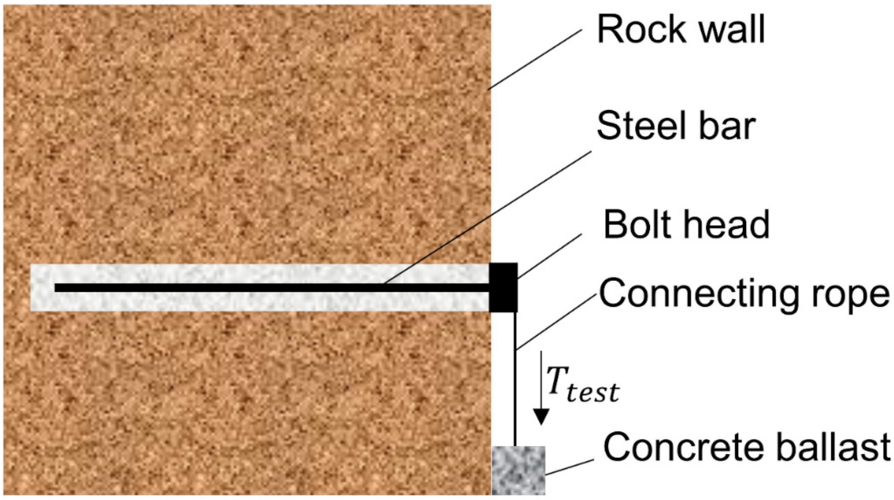

Fig. 10 Sketch of the transverse load test for the evaluation of the stiffness parameters k and β (not to scale).

After the lateral test, a strain-controlled pull-out test was performed to obtain the relation $N_{,test}$ - $\delta_{n,test}$, applying a 0.3 mm/sec pull rate. The test continued until the bolt was removed (i.e., failure of the bolt-rock interface) to evaluate the limit shear stress, τ_{lim}, on the lateral surface of the bolt:

$$\tau_{lim} = \frac{N_{slip,test}}{\pi \cdot \Phi_{hole,test} \cdot \mathrm{L}_{test}} \tag{40}$$

Where:

$N_{slip,test}$ is the force which causes the bolt-rock interface of the test bolt to fail (i.e. bolt slips away).

By carrying out bolt pull-out tests, it was possible to evaluate β_c as a function of the ratio between the applied axial force and the measured axial displacement (Oreste and Cravero, 2008):

$$\beta_c = \frac{1}{P_{hole,test} \cdot (EA)_{bolt,test} \cdot tanh^2\left(\sqrt{\frac{\beta_c \cdot P_{hole,test}}{(EA)_{bolt,test}}} \cdot L_{test}\right)} \cdot \left(\frac{N_{test}}{\delta_{n,test}}\right)^2 \tag{41}$$

Where:

L_{test} is the length of the tested bolt;

$\delta_{n,test}$ is the bolt head axial displacement due to the application of the axial force, N_{test};

$P_{hole,test}$ is the perimeter of the tested bolt; and

$(EA)_{bolt,test}$ is the axial stiffness of the tested bolt.

Given the form of the equation, a numerical solution was then carried out.

Experimental tests on a test bolt of 0.75 m length with a bar of 24 mm diameter and a thickness of the cementitious binder, t_{binder}, equal to 10 mm provided the following values:

- average lateral displacement $\delta_{t,test}$ of about 0.4 mm in the presence of a lateral force T_{test} of 0.75 tons;
- average axial displacement $\delta_{n,test}$ of about 0.1 mm in the presence of an axial force N_{test} of 1 ton; and
- a pull-out force $N_{slip,test}$ of 22 tons.

From the tests carried out it was possible to obtain the parameters k (8.9 MPa/mm), β_c (1.18 MPa/mm), and τ_{lim} (2.08 MPa). From these values, the remaining parameters necessary for the calculations were obtained for the different diameters of the steel bar, assuming L_a = 1.5 m (bolt length inside the block) and L_p = 2.5 m (anchoring length in the stable rock):

Φ_{bar}=20 mm: α =1.5966; β=11.7975; λ =12.31; χ =1.00797; ψ =1.008655; ω =0.99932;

Φ_{bar}=24 mm: α =1.3954; β=10.6492; λ =12.71; χ =1.01424; ψ =1.016135; ω = 0.99813;

Φ_{bar}=28 mm: α =1.2492; β=9.6936; λ =12.93; χ =1.02154; ψ =1.025507; ω =0.99613;

Φ_{bar}=32 mm: α =1.1377; β=8.8935; λ =13.02; χ =1.02933; ψ =1.036320; ω =0.99325;

Φ_{bar}=36 mm: α =1.0494; β=8.2178; λ =13.05; χ =1.03720; ψ =1.048177; ω =0.98953.

Finally, using equations 28 and 29, with σ_{yield} = 400 MPa and $F_{s,adm,yield}$ = $F_{s,adm,slip}$ = 1.25, we obtained the trend of stabilising forces shown in Fig. 11A and 11B.

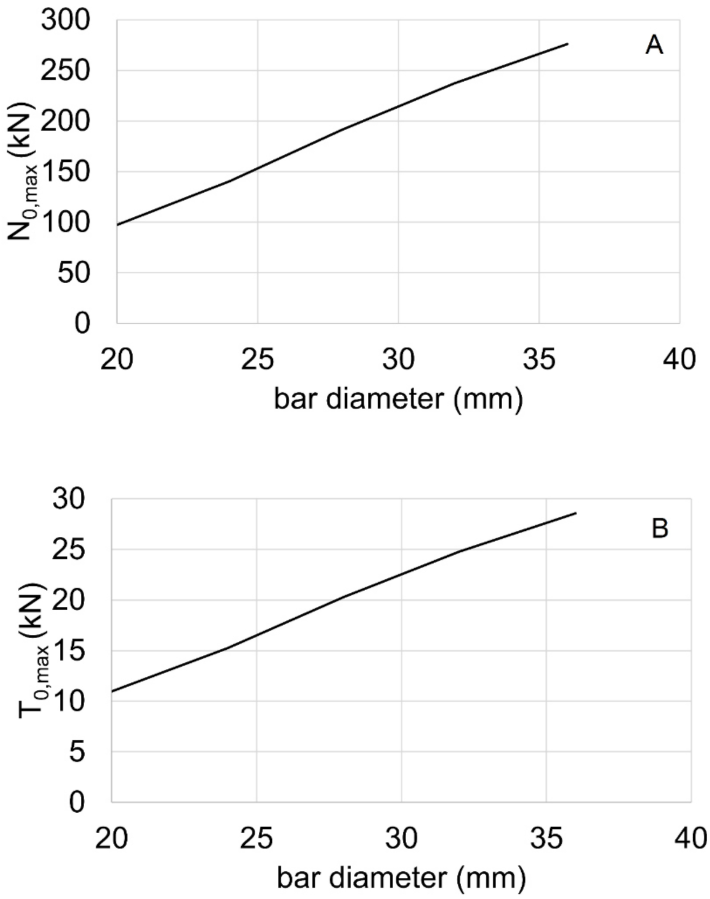

Fig. 11 Trend of the axial stabilisation force ($N_{0,max}$) (A) and of the transverse stabilisation force $T_{0,max}$ (B) as the diameter of the steel bar varies for the case study.

Knowing the stabilising forces that each bolt is able to offer to the potentially unstable rock block, it is possible to design the bolting system (number and diameter of the bolts) needed to achieve the desired safety factor with regard to the block sliding.

Conclusions

The analysis of the behaviour of a passive bolt used to stabilise a potentially unstable rock block from sliding along one or more surfaces is complex and requires three-dimensional numerical modelling in the presence of specific interfaces that represent the discontinuity surfaces that isolate the block and the contact surfaces of the bolt from the surrounding rock. Using the Winkler springs approach to simulate the bolt-rock interaction in the transverse and axial directions, a numerical solution was created in order to manage the numerous unknowns in the problem.

Thanks to the identification of specific critical points during the operation of passive bolts (at the point of intersection with the lateral surface of the block) and to the knowledge of the variability of intervals typical of the influential parameters that characterise the bolt-rock interaction, it was possible to develop a mathematical model to obtain the two stabilising forces that the bolt applies to the potentially unstable block. This model was based on some simplified hypotheses that produce a negligible error thanks to an extensive parametric analysis that considers intervals of variability typical of the parameters influencing the problem. These stabilisation forces are, in fact, the forces that must be considered as the static contribution of the bolt to reach conditions stable enough to be deemed acceptable for the potentially unstable block. One force was directed in the axial direction of the bolt; the other in a direction perpendicular to the axis of the bolt and lying in the plane which included the axis of the bolt and the displacement vector of the rock block.

The equations obtained allowed us to quickly evaluate the extent of the stabilising forces as a function of the diameter of the steel bar and therefore made it possible to correctly design the bolting operation by defining the bolt diameter and the number of bolts needed to stabilise the block of rock. An example from a real case allowed us to apply the equations obtained and chart the trend of the stabilisation forces as the diameter of the bar constituting the bolt changed.

Conflict of interests

Authors declare they have no conflict of interest.

References

1. Aminaipour, F., 2012. The effect load transfer mechanism of fully grouted bolts, M.Sc Thesis, Department of mine, Islamic Azad University, Bafgh, Iran.
2. Aziz, N., Jalalifar, H., 2007. The role of profile configuration on load transfer mechanism of bolt for effective support. J. Mines Met. Fuels (Dec), 539–545.
3. Bawden, F.W. (2011). Ground Control Using Cable and Rock Bolting. In: Darling, P., Ed., SME Mining Engineering Handbook, Society for Mining, Metallurgy and Exploration Inc., Littleton, 616-617.
4. Blümel, M., Schweiger, H.F., Golser, H., 1997. Effect of rib geometry on the mechanical behavior of grouted rock bolts. World Tunneling Congress'97. In: 23rd General Assembly of the International Tunneling Association, Wien, pp. 6–7.
5. Changxing, Z., Xu, C., Youdong, M., Xulin, L. (2015). Modeling of grout crack of rockbolt grouted system. International Journal of Mining Science and Technology 25, 73–77.
6. Chang, X., Wang,G., Liang, Z., Yang, J., Tang C. (2017). Study on grout cracking and interface debonding of rockbolt grouted system. Construction and Building Materials 135, 665–673

7. Chappell, B.A., 1989. Rock bolts and shear stiffness in jointed rock mass. J. Geotech. Eng. 115, 2, 179-197, *https://doi.org/10.1061/(ASCE)0733-9410(1989)115:2(179)*.

8. Chen, J., Saydam, S., Hagan, P.C. (2015). An analytical model of the load transfer behavior of fully grouted cable bolts. Construction and Building Materials 101, 1006–1015.

9. Das, K., Deb, D., 2011. Analytical model for fully grouted rock bolts considering movements of rock joints. Third Indian Rock Conference by ISRMTT, 187–199.

10. DSI, 2015. Mechanical Anchors and Rebar Rock Bolts, *https://static1.squarespace.com/static/529f28d4e4b0cf8c82ff287b/t/52acf49be4b0e46ab625d265/1387066523589/DSI-ALWAG-Systems_Mechanical-Anchors-and-Rebar-Rock-Bolts.pdf*, last access December 1, 2021.

11. Ferrero, M. (1995). The shear strength of reinforced rock joints. International Journal of Rock Mechanics and Mining Sciences & Geomechanics Abstracts, 32, 6, 595-605.

12. Ghadimi, M., Shahriar, K., Jalalifar, H. (2015). Tunnelling and Underground Space Technology, 50, 143-151.

13. Lancellotta, R., and Cavalera, J. (1999) Fondazioni. Mc Graw Hill, Milano

14. Lang TA (1961) Theory and practice of rock bolting. Trans Soc Min Engrs Am Inst Min Metall Petrolm Engrs 220: 333–348.

15. Li, C.C. (2017). Principles of rockbolting design. Journal of Rock Mechanics and Geotechnical Engineering. 9, 396-414.

16. Littlejohn,G.S., Bruce, D.A. (1977). Rock Anchors-State of the Art. Foundation Publications Ltd. Brentwood, UK.

17. Nie, W., Zhao, Z.Y., Ning, Y.J., and Guo, W. (2014). Numerical studies on rockbolts mechanism using 2D discontinuous deformation analysis. Tunnelling and Underground Space Technology, 41, 223–233.

18. Oreste, P.P., and Cravero, M. (2008). An analysis of the action of dowels on the stabilization of rock blocks on underground excavation walls. Rock Mechanics and Rock Engineering, 41(6), 835–868, DOI 10.1007/s00603-008-0162-2.

19. Oreste PP, Dias D (2012) Stabilisation of the excavation face in shallow tunnels using fibreglass dowels. Rock Mechanics Rock Eng., 45(4): 499-517. DOI: 10.1007/s00603-012-0234-1

20. Oreste, P.P. (2009). Face stabilisation of shallow tunnels using fibreglass dowels. Proceedings of the Institution of Civil Engineers-Geotechnical Engineering, 162, GE2, 95–109, doi: 10.1680/geng.2009.162.2.95.

21. Oreste, P (2013). Face stabilization of deep tunnels using longitudinal fibreglass dowels. International Journal of Rock Mechanics and Mining Sciences, 58, 127-140, *https://doi.org/10.1016/j.ijrmms.2012.07.011*.

22. Oreste, P., Spagnoli, G., Buccoleri, A.G. (2020). A parametric analysis on the influence of the binder characteristics on the behaviour of passive rock bolts with the Block Reinforcement Procedure. Geotechnical and Geological Engineering, *https://doi.org/10.1007/s10706-020-01285-7.*

23. Osgoui, R.R., Oreste P. (2007). Convergence-control approach for rock tunnels reinforced by grouted bolts, using the homogenization concept. Geotechnical and Geological Engineering, 25, 431–440, https://doi.org/10.1007/s10706-007-9120-0.

24. Ranjbarnia, M., Fahimifar, A., Oreste, P. (2014). A simplified model to study the behavior of pre-tensioned fully grouted bolts around tunnels and to analyze the more important influencing parameters. Journal of Mining Science, 50 (3), 533-548.

25. Ranjbarnia M, Fahimifar A, Oreste P (2016) Practical Method for the Design of Pretensioned Fully Grouted Rockbolts in Tunnels. Int J Geomech 16(1): https://doi.org/10.1061/(ASCE)GM.1943-5622.0000464.

FIGURE CAPTION

Fig. 1 Sketch of a passive rock bolt.

Fig. 2 Schematic representation of the potentially unstable rock block and the passive bolt (not to scale). L_a and L_p are the lengths of the bolt inside the potentially unstable rock block (zone I) and in the stable rock (zone II), respectively, ϑ is the angle of the block displacement vector with the direction of the axis of the passive bolts.

Fig. 3 Trend of the parameter λ by changing α for different values of β. A) Bar diameter 20 mm; B) Bar diameter 28 mm; C) Bar diameter 36 mm.

Fig. 4 Trend of the parameter χ by changing α for different values of L_a (bolt section in the potentially unstable rock block) and L_p (bolt section in stable rock).

Fig. 5 Trend of parameter ψ by changing α for different values of L_a (bolt section in the potentially unstable rock block) and L_p (bolt section in stable rock). The line with L_a=1.5 m and L_p=2.5 m overlaps the line with L_a=2.5 m and L_p=1.5 m.

Fig. 6 Trend of the parameter ω for L_a=0.5 m (bolt section in the potentially unstable rock block) and different values of L_p (bolt section in stable rock).

Fig. 7 Trend of the parameter ξ by varying λ for different values of angle ϑ.

Fig. 8 Trend of the parameter η by varying λ for different values of angle ϑ.

Fig. 9 Trend of the parameter ρ by varying λ for different values of angle ϑ.

Fig. 10 Sketch of the transverse load test for the evaluation of the stiffness parameters k and β (not to scale).

Fig. 11 Trend of the axial stabilisation force ($N_{0,max}$) (A) and of the transverse stabilisation force $T_{0,max}$ (B) as the diameter of the steel bar varies for the case study.